Article

Preparation and Magneto-Structural Investigation of High-Ordered (L2₁ Structure) Co₂MnGe Microwires

Mohamed Salaheldeen [1,2,3,4,*] , Asma Wederni [1,2,4] , Mihail Ipatov [1,2] , Valentina Zhukova [1,2,4] and Arcady Zhukov [1,2,4,5,*]

1 Departamento de Polímeros y Materiales Avanzados, Facultad Química, Universidad del País Vasco, UPV/EHU, 20018 San Sebastián, Spain; asma.wederni@ehu.eus (A.W.)
2 Departamento de Física Aplicada, EIG, Universidad del País Vasco, UPV/EHU, 20018 San Sebastián, Spain
3 Physics Department, Faculty of Science, Sohag University, Sohag 82524, Egypt
4 EHU Quantum Center, University of the Basque Country, UPV/EHU, 20018 San Sebastián, Spain
5 IKERBASQUE, Basque Foundation for Science, 48011 Bilbao, Spain
* Correspondence: mohamed.salaheldeenmohamed@ehu.eus (M.S.); arkadi.joukov@ehu.eus (A.Z.)

Abstract: We used the Taylor–Ulitovsky technique to prepare nanocrystalline Co₂MnGe Heusler alloy glass-coated microwires with a metallic nucleus diameter of 18 ± 0.1 μm and a total diameter of 27.2 ± 0.1 μm. Magnetic and structural studies were carried out to determine the fundamental magneto-structural characteristics of Co₂MnGe glass-coated microwires. XRD revealed a well-defined nanocrystalline structure with an average grain size of about 63 nm, lattice parameter a = 5.62 and a unique mixture of L2₁ and B2 phases. The hysteresis loops measured at different temperatures indicated a well-known ferromagnetic behavior for the reduced remanent, where a monotonic increasing in the reduced remanent and saturation magnetization occurs. The coercivity shows anomalous behavior compared to the Co2Mn-based glass-coated microwires. The magnetization curves for field cooling and field heating (FC–FH) demonstrate a considerable dependence on the applied magnetic field, ranging from 50 Oe to 20 kOe. Internal stresses, originated by the production process, resulted in various magnetic phases, which were responsible for the notable difference of FC and FH curves on magnetization dependence versus temperature. Furthermore, the ferromagnetic behavior and expected high Curie temperature, together with high degree of the L2₁ order, make it a promising candidate for many applications.

Keywords: microwires; Heusler alloys; magneto-structural characterization; secondary phases; L2₁ and B2 phases structure

1. Introduction

The unique properties of nano/microstructured magnetic materials have sparked significant interest in the field of materials science and engineering. These materials possess high magnetic anisotropy, which is further enhanced by the presence of nanoscale or microscale structures. As a result, they have found numerous applications in various fields, such as data storage, energy conversion, biomedicine, and sensing [1–7].

Heusler alloys, discovered at the beginning of the 20th century, are a diverse family of binary, ternary, and quaternary compounds with a wide range of physical characteristics suitable for various applications, including spintronics, magnetic refrigeration, and actuators, among others [8,9]. They stimulate the curiosity of fundamental and applied researchers due to their considerable tunability depending on chemical composition, crystal structure, or electronic structure [10]. Spin polarization, superconductivity, shape memory, and magnetocaloric effect, in particular, have attracted considerable interest from both an experimental and theoretical point of view [8–10]. Heusler alloys, also known as full-Heusler alloys with the stoichiometry X₂YZ, may be classified into many classes based on their chemical composition and consequent characteristics [11]. Heusler based on Co₂YZ is

a prominent category of materials with high spin polarization (P) or even half metallicity (P 100%). However, theoretical and experimental investigations show that spin polarization is very sensitive to structural instability. The $L2_1$ crystalline phase has the greatest structural ordering, which is necessary to achieve the requisite spin polarization levels. While the mutual exchange of atoms on the Y–Z position (B2 disorder) has little effect on spin polarization values, the X–Y or X–Y–Z disorders (D03 or A2, respectively) can dramatically reduce spin polarization [12]. Moreover, the Heusler alloys described above, have complex crystalline structures that need extremely high temperatures (usually >1000 K in the bulk form and >650 K in the thin-film form) for their crystalline ordering [13]. As a result, one major issue when producing X_2YZ full-Heusler thin films is to achieve the chemically ordered $L2_1$ phase, as the excellent features of Co_2-based Heusler compounds (Co_2MnGe) are most typically expected for this $L2_1$ phase (see Figure 1a). Co_2-based Heusler alloys, on the other hand, can crystallize in a variety of phases with reduced chemical ordering, without affecting the atomic sites in the lattice [14]. The most common disordered phase is B2, in which the Y and Z atoms are randomly distributed, resulting in a primitive unit cell rather than the FCC cell (Fm-3m→Pm-3m) (see Figure 1b). At this time, it is unknown how much the chemical disproportion affects the physical features. It is worth noting that ab initio calculations [15] and experiments [16] show that the physical properties (Curie temperature, cell parameter, magnetic moment, magnetic damping constant, and spin polarization at EF) of the $L2_1$ and B2 phases are slightly distinguishable from one another, and the half-metallic spin gap should be conserved.
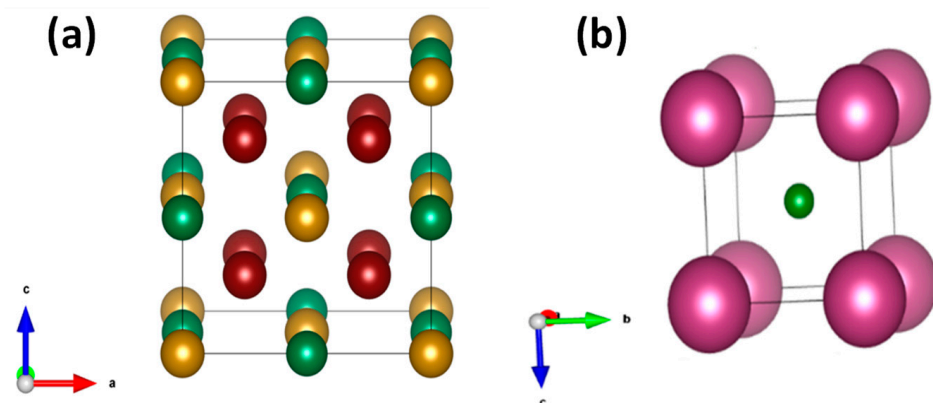

Figure 1. (**a**) $L2_1$ cubic structure (Co atoms occupy the red positions, Mn atoms occupy the yellow positions and Ge atoms occupy the green positions) and (**b**) B2 cubic structure (Co atoms occupy the purple positions, Mn and Ge atoms occupy the green positions).

The half- and full-metallic Heusler alloys prepared by physical vapor deposition, i.e., thin-film forms, ball milling, or arc melting, are critical for obtaining the necessary structural ordering, i.e., $L2_1$, and preventing the formation of disordered structures, such as B2, A2, and DO3, which may arise during the alloy manufacturing process [9]. Several of them continue to face challenges, such as easy oxidation from the standpoint of appropriate atomic ordering, high cost of preparation processes, chemical composition inhomogeneity, and lattice mismatch between the alloy and the substrate [9,10]. Long annealing durations at high temperatures are utilized to avoid the creation of unnecessary phase structures. To address the aforementioned shortcomings, Heusler alloy manufacture has recently used a rapid quenching technique [10]. The fast quenching approach has the benefit of allowing for the fabrication of diverse amorphous and crystalline materials in varied shapes, such as ribbons and microwires, in a single step [12].

Studies of magnetic wires have attracted substantial attention along several decades [17]. The main attention is paid to amorphous magnetic wires, which can present unique magnetic properties, such as spontaneous magnetic bistability or giant magnetoimpedance (GMI) effects [17,18]. Magnetic wires with amrohpous and/or nanocrstalline can be pre-

pared using various fabrication methods involving rapid solidification [17,18]. However, only the so-called Taylor–Ulitovsky fabrication method allows for the preparation of the magnetic microwires with the most extended (from 0.2 up to 100 μm) diameters, *d*, range [17,18]. Such microwires are composites consisting of a metallic nucleus (with $0.2 \leq d \leq 100$ μm), usually comprising iron, cobalt, nickel or their alloys, covered by thin, flexible, and insulating glass (typically Pyrex or Duran) coating (typically with a thickness of 0.5 to 10 μm) [17,18]. Accordingly, glass-coated microwires have extended potential applications in sensing, actuation, and biomedical engineering. The glass coating provides exceptional mechanical stability to the microwires, while also protecting them from corrosion, oxidation, and other environmental conditions. Furthermore, the magnetic softness of the amorphous metallic nucleus, together with the glass coating, enables high sensitivity to external stimuli such as magnetic fields, temperature changes, and mechanical stress [17–24]. Such sensitivity is related to the metallic nucleus magneto-strictive origin, which responds to the applied stimulus. Glass-coated microwires have been utilized to create innovative sensors that measure magnetic fields, temperature, and stress for a variety of applications [17–19]. They have also demonstrated promising features for actuators and in medicinal applications, including medication delivery and cancer therapy. The unique mix of qualities of glass microwires makes them a viable material for future technological improvements [17,19].

In the current work, we present an attempt to obtain Co_2MnGe glass-coated microwires. The fabrication method choice is due to the interesting magneto-structural behavior of glass-coated microwires from Heusler alloys, as well as functional properties of glass-coated microwires, such as superior mechanical properties, insulating, thin and flexible glass-coating, and thin dimensionality [19–27]. Accordingly, we manufactured Co_2MnGe glass-coated microwires using the Taylor–Ulitovsky process, described in details elsewhere [20,21]. The Taylor–Ulitovsky technique, known since the 1960s [28], is one of the fabrications recently used to produce Heusler alloys glass-coated microwires [19–27]. The fundamental advantage of this low-cost technology is that it enables the manufacturing of thin and long (a few kilometers long) microwires with an extended diameter range (d-values from 0.1 to 100 μm) at high speeds (up to a few hundred meters per minute) [28–30]. Glass-coated microwires with outstanding mechanical characteristics are also produced using this technology [21,31–33]. The glass coating on the microwires can provide us additional benefits, such as increased insulation and environmental protection. Furthermore, the availability of a biocompatible thin, flexible, insulating, and highly transparent glass covering might help biological applications [34,35]. As a result, Heusler microwires based on Co_2MnGe are a potentially smart material for a wide variety of device applications. To the best of our knowledge, no one has reported on the preparation, and structural, mechanical, or magnetic characterization of Co_2MnGe-based glass-covered Heusler microwires.

2. Materials and Methods

For the production of Co_2MnGe glass-coated microwires, the first step is the manufacturing of the Co_2MnGe alloy ingot by arc melting under argon atmosphere. The melting process starts by melting the nominal elements with high purity (Co (99.99%), Mn (99.9%) and Ge (99.9%)). The argon atmosphere is proceeded in order to avoid the oxidation during melting. To attain an alloy with higher homogeneity, the melting route was repeated five times. Then, the nominal composition was verified by performing energy-dispersive X-ray (EDX) analysis, finding the real composition to be $Co_{55}Mn_{22}Ge_{23}$. Afterwards, when we acquired the alloy, we prepared the Co_2MnGe glass-coated microwires using the Taylor–Ulitovsky technique [20,21,28]. This fabrication procedure consists of melting the previously prepared alloy inside the glass tube with a high-frequency inductor, the forming of the glass capillary, and drawing the composite (metallic nucleus cover by glass) microwire directly from the melted master alloy. During the drawing phase, the molten metallic alloy fills the glass capillary and then a glass-coated microwire is formed [17,18,29]. Finally, the metallic nucleus of the microwire is completely covered by an insulating, flexible, and

continuous glass-coating. The chemical composition of the metallic nucleus is provided in Table 1. The obtained diameter of the inner metallic nucleus of the microwire sample is around 18 μm, while the total diameter (with an external Pyrex coating) is around 27.1 μm. The microstructure and phase composition analysis for the produced samples have been examined with a BRUKER X-ray diffractometer (D8 Advance, Bruker AXS GmbH, Karlsruhe, Germany), performed with Cu Kα (λ = 1.54 Å) radiation. Furthermore, the magnetic behavior was scrutinized through the magnetization curves, which were measured using a PPMS (Physical Property Magnetic System, Quantum Design Inc., San Diego, CA, USA) vibrating sample magnetometer at temperatures, T, between 5 and 400 K. A magnetic field, H, between 50 Oe and 20 kOe, was applied along the sample axis and perpendicular to the wire axis. The results are provided in terms of the normalized magnetization, M/M_{5K}, where M_{5K} is the magnetic moment obtained at 5 K.

Table 1. Atomic percentage of Co, Mn, and Ge elemental composition in Co_2MnGe glass-coated microwires.

EDX Spectrum	Co (at. %)	Mn (at. %)	Ge (at. %)
Average	53 ± 2	22 ± 2	25 ± 1

3. Results

To check the chemical composition of the Co_2MnGe glass-coated microwires, we performed EDX/SEM analysis and the output results are listed in Table 1. The composition of the metallic nucleus was found to be somewhat different from the stoichiometric one using the EDX data from Table 1 (Co_2MnGe). This little variance was due to the peculiarities of the preparation procedure, which included alloy melting and casting. We examined the nominal composition for 10 locations to determine the amount of difference. The actual 2:1:1 ratio for Co, Mn, and Ge was verified for all locations, with an atomic average $Co_{56}Mn_{19}Ge_{25}$.

X-ray diffraction (XRD) patterns of Co_2MnGe alloys in glass-coated microwires were investigated at room temperature and are shown in Figure 2. As shown in Figure 2, at low angles within the XRD diffractogram, at $2\theta \approx 22°$, a huge halo is observed, which must be ascribed to the amorphous glass coating presence. The same behavior was reported and discussed elsewhere [19–26]. The Co_2MnGe full-Heusler alloy has to be indexed in the Fm-3m space group with an $L2_1$ cubic structure. Indeed, the cubic structure of Co_2MnGe was confirmed by the XRD profile. From the XRD pattern analysis, the presence of a cubic structure is well perceived. Nevertheless, a second phase can be detected (see Figure 2b). This hypothesis is drawn from the fact that the main peak (220) results from an overlapping of two very close peaks; one peak at around $2\theta \approx 44°$, recognized as the $L2_1$ structure, and the other one at about $2\theta \approx 45°$, which may be due to the B2-type disordered structure.

Therefore, the crystalline structure of the prepared Co_2MnGe glass-coated microwires is an FCC-$L2_1$, with a minor BCC-B2 cubic structure in some parts of the synthesized sample. The estimation of the volume fraction of the obtained microstructure phase, i.e., $L2_1$ and B2, prove that the main phase of the as-prepared Co_2MnGe glass-coated microwires is FCC-$L2_1$, with percentages of 92.3 and 7.7% for B2 type. However, the low value of the disordered microphase structure, i.e., B2, changing in magnetic behavior has been observed, as will be illustrated in the magnetic section. Although the $L2_1$ structure is an extremely ordered and crucial structure to achieve the required spin polarization values, it should be mentioned that the manufacturing process of the microwires may result in a different structural disorder (B2, A2, DO3, etc.), as described in the introduction. For instance, the mutual disorder between Y (Mn) and Z (Ge) atomic positions outlines the B2 disorder type (see Figure 1). It is worth noting that the theoretical calculations account for the fact that the B2-type disorder structure produced in Y–Z elements has a far smaller impact on the spin polarization values than the X–Y disorder and X–Y–Z disorder, both of which noticeably diminish this feature [12]. The presence of (111), (200), and (311) super-lattice diffraction peaks confirms the presence of the high-ordered $L2_1$ structure [36].

The estimated lattice parameter and calculated volume of the cell are a = 5.7430 Å and V = 189.42 Å^3, respectively, which perfectly matched with the lattice parameter and volume values reported elsewhere [16,37] for Co$_2$MnGe thin films. In addition, we estimated the lattice parameters of the cell for the secondary phase of B2 type, which were about a = 4.28 A^0 and V = 78.40 Å^3. Such a high-ordered L2$_1$ structure is detected in Co$_2$MnGe-based glass-coated microwires for the first time.

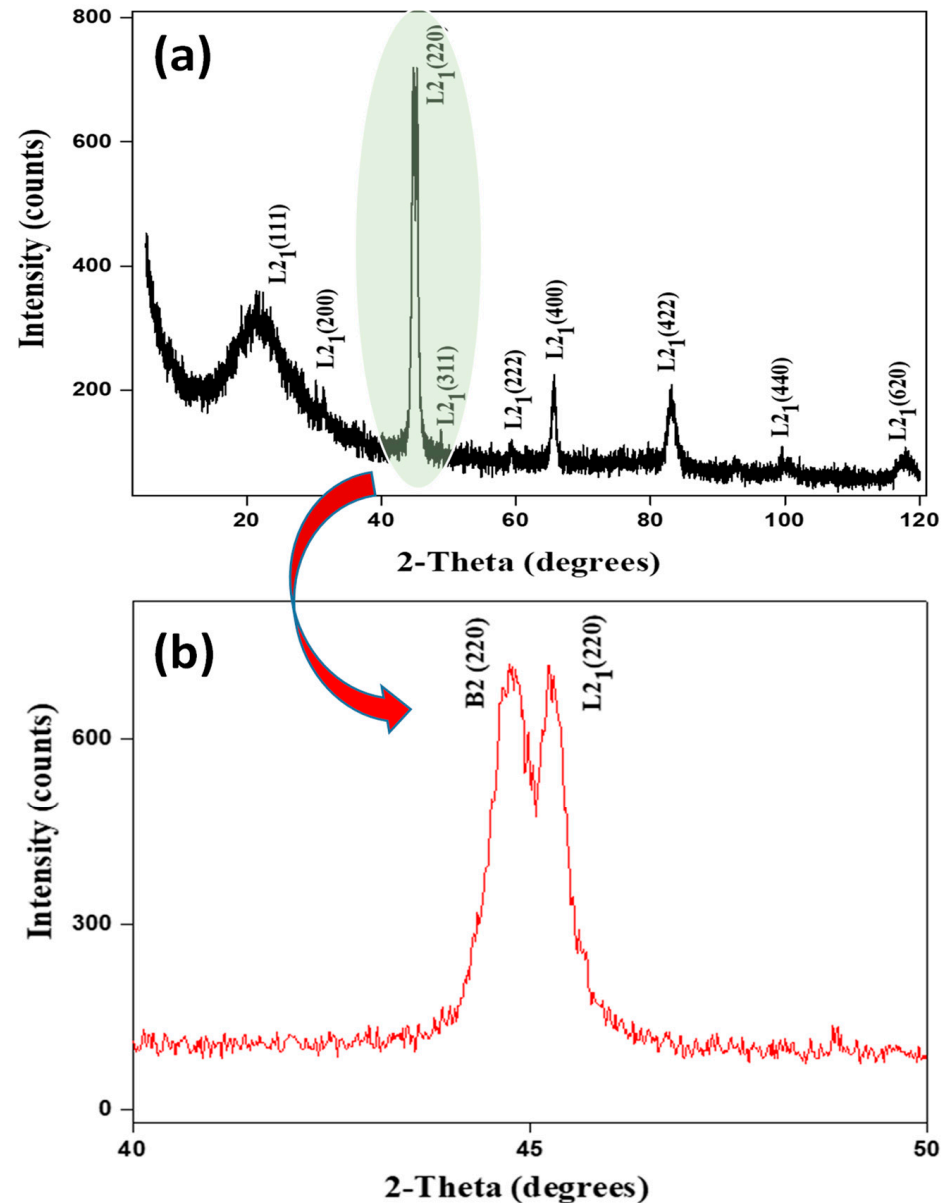**Figure 2.** (**a**) X-ray diffraction (XRD) diffractograms at room temperature of Co$_2$MnGe, and (**b**) XRD diffraction patterns of Co$_2$MnGe (enlargement of (220) peaks).

For a deeper investigation of the microstructure of Co$_2$MnGe, we used the Debye-Scherrer's equation, described in our previous works [23]. Using this protocol, we can estimate the average grain size, D$_g$, related to the main peak, i.e., L2$_1$ cubic structure, being about 63.3 nm for the as-prepared Co$_2$MnGe microwires.

The ferromagnetic ordering of the as-prepared Co$_2$MnGe glass-coated microwires is evidenced in Figure 3, where the magnetic hysteresis (MH) loops measured at 5 K ≤ T ≤ 305 K are provided. The MH loops have been measured at an applied high magnetic field, H, of up to ±40 kOe, to make sure that the Co$_2$MnGe glass-coated microwire sample presented magnetic saturation. In addition, MH loops were measured at different temperatures to illustrate their

behavior with temperature. Due to the high-ordered $L2_1$ structure, perfect ferromagnetic behavior is observed where the normalized saturation magnetization has a monotonic increase by decreasing the temperature, i.e., the lowest value of the M/M_{5K} ratio was detected at 305 K and the highest value was observed at 5 K. Thus, the high degree of the $L2_1$ ordered phase of the as-prepared, as well as the average grain size, D_g, of Co_2MnGe glass-coated microwires are relevant factors that can affect MH behavior with temperature. Such a characteristic of MH loops by varying the temperature was not observed in our previous investigation for the Co_2Mn-based glass-coated microwires, due to the low degree of the $L2_1$ ordered phase (see [20,25]).
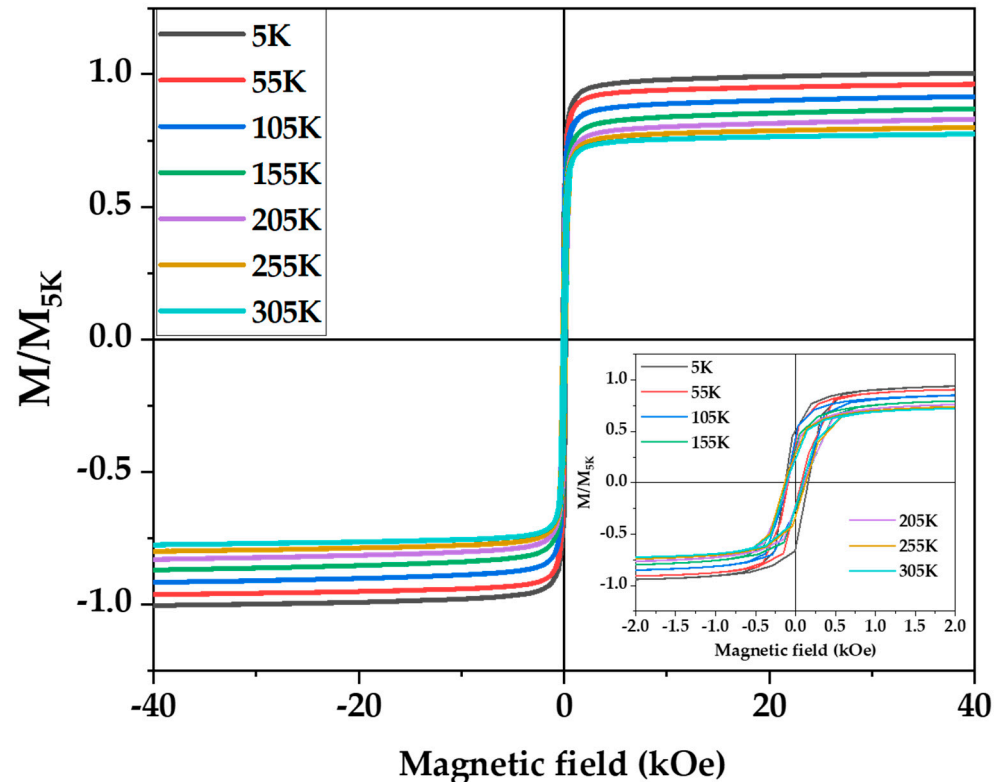

Figure 3. Magnetization curves M/M_{5K} (H) of the as-prepared Co_2MnGe glass-coated microwires measured at a maximum field, ±40 kOe, and a temperature range of 305 K to 5 K. Low field M/M_{5K} (H) loops are shown in the inset.

From low-field hysteresis loops (see the inset of Figure 3) the coercivity, H_c, of about 125 Oe for the whole T-range can be appreciated. Such H_c values are about one order of magnitude higher than that reported for other Co_2Mn-based microwires [20,25]. This difference in H_c values can be related to higher average D_g values observed in the as-prepared Co_2MnGe glass-coated microwires.

To understand the relationship between the temperature and the magnetic parameters, such as H_c and normalized reduced remanent M_r, these variables are obtained directly from the MH loops that were measured at various temperatures. Figure 4 illustrates the non-monotonic H_c behavior when H_c increases from 103 Oe to 120 Oe, as the temperature decreases from 305 K to 150 K. Then, when the temperature decreases from 155 K to 55 K, H_c starts to decrease from 120 Oe to 97 Oe. The maximum value of H_c is reported at T = 5 K, while a rapid rise in H_c has been seen below T = 55 K. Such behavior of the H_c is totally different from the H_c behavior of Co_2MnSi glass-coated microwires, where the coercivity shows a stable behavior with temperature, as reported by [20,25]. The variation in H_c with temperature is strongly related to the microstructure evolution, as glass-coated microwires are very sensitive to the magnetic field and temperature. In addition, strong internal stress introduced during the fabrication of glass-coated microwires is the

primary factor in the unusual change of the axial coercivity of Heusler-based glass-coated microwires [21,26]. Moreover, temperature has a significant impact on internal stresses. As described in the structural section of this publication, the Co_2MnGe glass-coated microwires studied in this paper had $L2_1$ and B2 microstructures. However, the B2-BCC microstructure has a low volume fraction of about 7.7%, while the main volume fraction corresponds to the $L2_1$ FCC structure (92.3%). Such a disorder microstructure can affect the behavior of the coercivity, especially at a low magnetic field, as described by the thermomagnetic properties at the low field (Figures 5 and 6). These features affect the behavior of the temperature dependence of coercivity. For the M_r and saturation magnetization (M_s) dependencies in temperature, normal ferromagnetic behavior is observed, where the M_r and M_s show a monotonic increase by decreasing the temperature from 305 K to 5 K, as described in Figure 4.
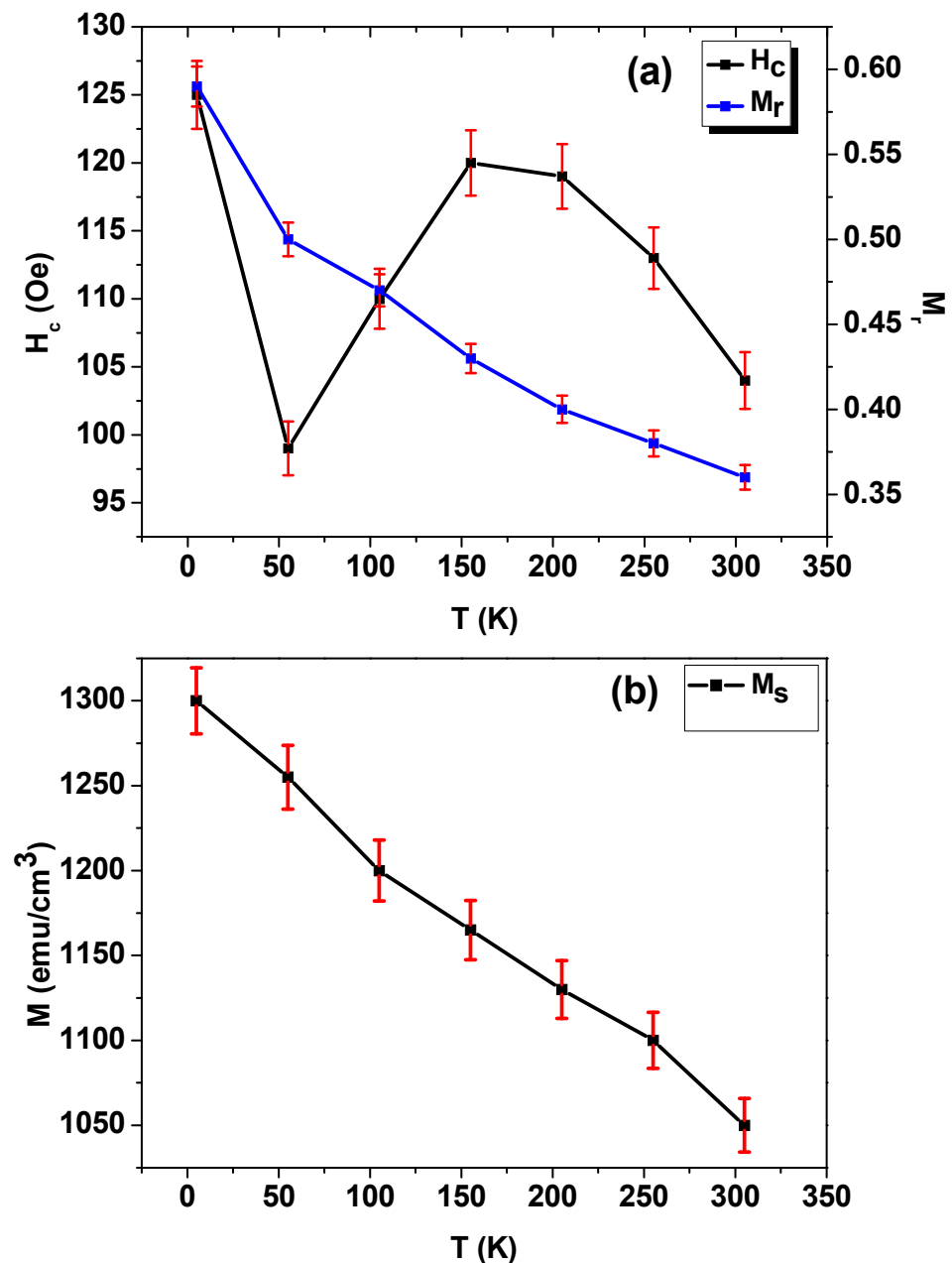

Figure 4. Coercivity (H_c) and normalized remanent (M_r) (**a,b**) magnetization saturation (M_s) of the as-prepared Co_2MnGe glass-coated microwire dependence on temperature.
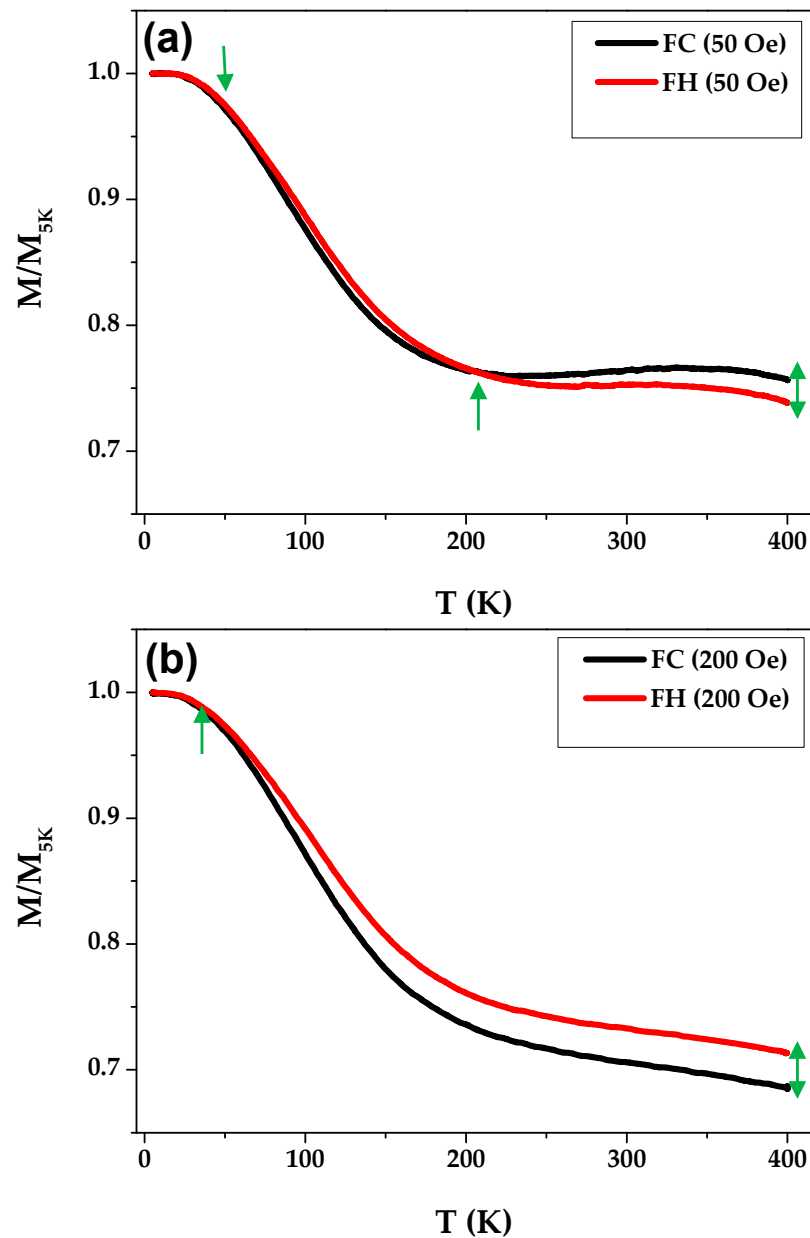
Figure 5. Measured temperature dependence on magnetization for the as-prepared Co_2MnGe glass-coated microwires, with 50 Oe (**a**) and 200 Oe (**b**) of applied external magnetic field.

The thermomagnetic properties, i.e., M/M_{5K} vs. T, and magnetic field of the Co_2MnGe glass-coated microwires, are shown in Figures 5 and 6. In this part, we only focused on the magnetization behavior at a wide range of temperatures and magnetic fields to evaluate the possible magnetic phase transition. We measured temperature dependencies of the magnetization in the temperature, T, range from 5 to 400 K. To avoid the over estimation of the magnetization, we used normalized magnetization parameters (M/M_{5K}), where the M_{5K} is the highest magnetic moment detected at 5 K. Notable ferromagnetic behavior has observed for all ranges of measured temperatures and applied magnetic fields, which is expected due to the high Curie temperature for the Co_2MnGe alloy above 883 K [16,37]. For field cooling (FC) and field heating (FH) magnetization curves, a notable mismatching between FC and FH curves has been observed when (M/M_{5K} vs. T) the dependence was measured at a low magnetic field, i.e., 50 Oe and 200 Oe, as seen in Figure 5. For the M/M_{5K} (T) curves measured at 50 Oe, the FC curve overlapped FH curves at a temperature range of 400 K to 200 K, then reversed at a temperature range of 200 K to 30 K. Finally, full matching

was observed for T below 30 K. This behavior can be discussed with two flipped points, where the FC and FH magnetization curves changed. By increasing the externally applied magnetic field, i.e., 200 Oe, these flipping points disappeared and a uniform magnetic tendency was detected, where FH overlapped FC for the temperature range of 400 K to 20 K, while perfectly matching below 20 K, as indicated in Figure 5b.
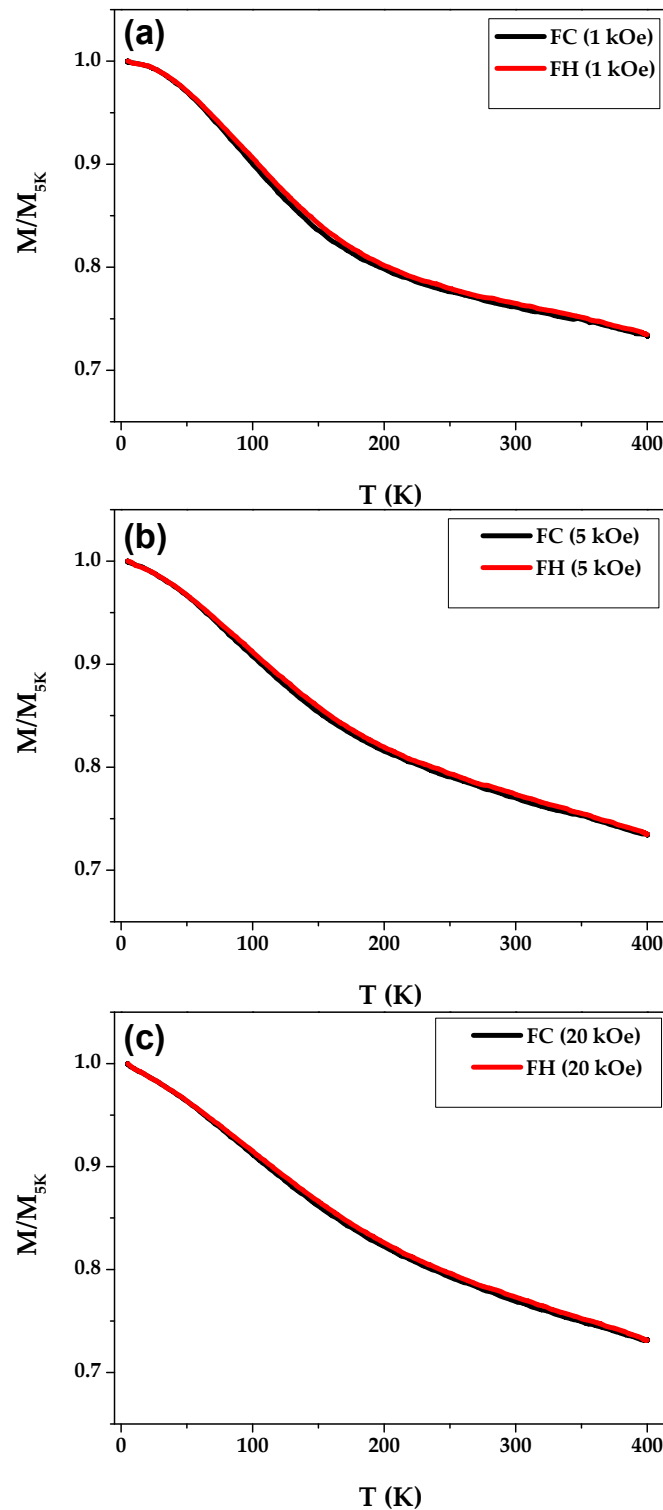

Figure 6. Measured temperature dependence of magnetization for the as-prepared Co$_2$MnGe glass-coated microwires, with 1 kOe (**a**), 5 kOe (**b**), and 20 kOe (**c**) of applied external magnetic field.

For further increase of the applied magnetic field, both the FC and FH magnetization curves were perfectly matched and homogenous ferromagnetic behavior was seen (see Figure 6). The interesting magnetic field dependence of FC and FH curves indicates the sensitivity of Co_2MnGe to the magnetic field and temperature.

4. Discussion

The strong variation of the FC and FH magnetization curves with externally applied magnetics field must be related to the microstructure of the Co_2MnGe glass-coated microwires and the peculiarities of the fabrication method. As illustrated in XRD analysis, the high-ordered $L2_1$ microstructure is confirmed alongside the disordered B2 phase structure. The existence of the B2 disorder phase structure strongly affects the magnetic behavior at applied low magnetic fields, i.e., 50 and 200 Oe, resulting in the two flipped points and the mismatching between the FC and FH magnetization curves. This disordered effect is totally suppressed by applied high magnetic fields of 1 kOe (in our case) to 20 kOe. Thus, a perfect matching of FC and FH magnetization curves was observed (see Figure 6). The increase in the degree of microstructure ordering of Heusler-based glass-coated microwires leads to a uniform magnetic behavior with temperature and magnetic field (for more details see [19,24–27]). The origin of such a disordered structure must be related to the rapid melt quenching involved in the fabrication method, as well as by the internal stresses related to the composite origin of glass-coated microwires [23,27,38–40]. Alongside the disordered structure, the preparation of glass-coated microwires is also characterized by large internal stresses (up to 1 GPa), originating mainly from the essentially different thermal expansion coefficients of the metallic alloy and glass-coating [38–40]. On the other hand, such disordered structures have also been observed in thin films [41]. It is worth mentioning that the structural disorder and high internal stresses in glass-coated Heusler alloy microwires and thin films can be considerably diminished by appropriate annealing [41,42]. Therefore, one of the future lines of research of Co_2MnGe glass-coated microwires will concern with the search for appropriate postprocessing for magnetic property tunning.

5. Conclusions

In summary, we report on the fabrication of high-ordered Co_2MnGe glass-coated microwires by using the Taylor–Ulitovsky technique. In the as-prepared Co_2MnGe microwires, ferromagnetic ordering is observed in a whole range of temperatures. The XRD analysis confirms the presence of high-ordered nanocrystalline $L2_1$ structure, with an average of crystallite size of 63.3 nm and lattice constant of 5.7430. In addition to the $L2_1$ structure, a disordered B2 structure is found, combining with the main peak of $L2_1$. The estimation of the volume fraction for the main and secondary phase indicated the majority being the $L2_1$ FCC structure, with 92.3% and 7.3% for the B2-BCC structure. The coercivity shows an irregular tendency regarding temperature, where the two flipped points, when tendency is changed, are detected. The existence of a B2 disordered structure can explain the mismatching of FC and FH magnetization curves and the anomalous coercivity tendency with temperature. By increasing the externally applied field, the effect of disordered the B2 microstructure is totally suppressed and uniform magnetic behavior is seen for applied magnetic fields higher than 1 kOe. Future investigations are needed due to study the effect of high-ordered microstructures on different physical properties. The outcoming result reveals the promise of Co_2MnGe, with high-spin, polarized and $L2_1$-ordered structure, in multifunctional thermomagnetic application.

Author Contributions: Conceptualization, M.S. and A.Z.; methodology, V.Z. and M.I.; validation, M.S., V.Z. and A.Z.; formal analysis, M.S. and A.W.; investigation, M.S., A.W. and A.Z.; resources, V.Z. and A.Z.; data curation M.S., M.I. and A.W.; writing—original draft preparation, M.S., A.W. and A.Z.; writing—review and editing, M.S. and A.Z.; visualization, M.S., A.W. and V.Z. supervision, A.Z.; project administration, V.Z. and A.Z.; funding acquisition, V.Z. and A.Z. All authors have read and agreed to the published version of the manuscript.

References

1. Hoop, M.; Ribeiro, A.S.; Rösch, D.; Weinand, P.; Mendes, N.; Mushtaq, F.; Chen, X.Z.; Shen, Y.; Pujante, C.F.; Puigmartí-Luis, J.; et al. Mobile Magnetic Nanocatalysts for Bioorthogonal Targeted Cancer Therapy. *Adv. Funct. Mater.* **2018**, *28*, 1705920. [CrossRef]
2. Salaheldeen, M.; Vega, V.; Fernández, A.; Prida, V.M. Anomalous In-Plane Coercivity Behaviour in Hexagonal Arrangements of Ferromagnetic Antidot Thin Films. *J. Magn. Magn. Mater.* **2019**, *491*, 165572. [CrossRef]
3. Salaheldeen, M.; Nafady, A.; Abu-Dief, A.M.; Díaz Crespo, R.; Fernández-García, M.P.; Andrés, J.P.; López Antón, R.; Blanco, J.A.; Álvarez-Alonso, P. Enhancement of Exchange Bias and Perpendicular Magnetic Anisotropy in CoO/Co Multilayer Thin Films by Tuning the Alumina Template Nanohole Size. *Nanomaterials* **2022**, *12*, 2544. [CrossRef] [PubMed]
4. Salaheldeen, M.; Martínez-Goyeneche, L.; Álvarez-Alonso, P.; Fernández, A. Enhancement the Perpendicular Magnetic Anisotropy of Nanopatterned Hard/Soft Bilayer Magnetic Antidot Arrays for Spintronic Application. *Nanotechnology* **2020**, *31*, 485708. [CrossRef] [PubMed]
5. Skjærvø, S.H.; Marrows, C.H.; Stamps, R.L.; Heyderman, L.J. Advances in artificial spin ice. *Nat. Rev. Phys.* **2019**, *2*, 13–28. [CrossRef]
6. Maniv, E.; Murphy, R.A.; Haley, S.C.; Doyle, S.; John, C.; Maniv, A.; Ramakrishna, S.K.; Tang, Y.-L.; Ercius, P.; Ramesh, R.; et al. Exchange bias due to coupling between coexisting antiferromagnetic and spin-glass orders. *Nat. Phys.* **2021**, *17*, 525–530. [CrossRef]
7. Salaheldeen, M.; Abu-Dief, A.M.; Martínez-Goyeneche, L.; Alzahrani, S.O.; Alkhatib, F.; Álvarez-Alonso, P.; Blanco, J.Á. Dependence of the Magnetization Process on the Thickness of $Fe_{70}Pd_{30}$ Nanostructured Thin Film. *Materials* **2020**, *13*, 5788. [CrossRef]
8. De Groot, R.A.; Mueller, F.M.; Engen, P.G.V.; Buschow, K.H.J. New Class of Materials: Half-Metallic Ferromagnets. *Phys. Rev. Lett.* **1983**, *50*, 2024. [CrossRef]
9. Elphick, K.; Frost, W.; Samiepour, M.; Kubota, T.; Takanashi, K.; Sukegawa, H.; Mitani, S.; Hirohata, A. Heusler Alloys for Spintronic Devices: Review on Recent Development and Future Perspectives. *Sci. Technol. Adv. Mater.* **2021**, *22*, 235–271. [CrossRef]
10. Tavares, S.; Yang, K.; Meyers, M.A. Heusler alloys: Past, properties, new alloys, and prospects. *Prog. Mater. Sci.* **2023**, *132*, 101017. [CrossRef]
11. Bai, Z.; Shen, L.E.I.; Han, G.; Feng, Y.P. Data Storage: Review of Heusler Compounds. *Spin* **2012**, *2*, 1230006. [CrossRef]
12. Balke, B.; Wurmehl, S.; Fecher, G.H.; Felser, C.; Kübler, J. Rational Design of New Materials for Spintronics: Co_2FeZ (Z=Al, Ga, Si, Ge). *Sci. Technol. Adv. Mater.* **2008**, *9*, 014102. [CrossRef]
13. Hirohata, A.; Sagar, J.; Lari, L.; Fleet, L.R.; Lazarov, V.K. Heusler-alloy films for spintronic devices. *Appl. Phys. A* **2013**, *111*, 423–430. [CrossRef]
14. Bacon, G.E.; Plant, J.S. Chemical ordering in Heusler alloys with the general formula A_2BC or ABC. *J. Phys. F Metal. Phys.* **1971**, *1*, 524–532. [CrossRef]
15. Kumar, A.; Pan, F.; Husain, S.; Akansel, S.; Brucas, R.; Bergqvist, L.; Chaudhary, S.; Svedlindh, P. Temperature-dependent Gilbert damping of Co_2FeAl thin films with different degree of atomic order. *Phys. Rev. B* **2017**, *96*, 224425. [CrossRef]
16. Özduran, M.; Candan, A.; Akbudak, S.; Kushwaha, A.K.; İyigör, A. Structural, Elastic, Electronic, and Magnetic Properties of Si-Doped Co_2MnGe Full-Heusler Type Compounds. *J. Alloys Compd.* **2020**, *845*, 155499. [CrossRef]
17. Zhukov, A.; Corte-Leon, P.; Gonzalez-Legarreta, L.; Ipatov, M.; Blanco, J.M.; Gonzalez, A.; Zhukova, V. Advanced Functional Magnetic Microwires for Technological Applications. *J. Phys. D Appl. Phys.* **2022**, *55*, 253003. [CrossRef]
18. Chiriac, H.H.; Ovari, T.A. Amorphous glass-covered magnetic wires: Preparation, properties, applications. *Prog. Mater. Sci.* **1996**, *40*, 333–407. [CrossRef]
19. Mitxelena-Iribarren, O.; Campisi, J.; de Apellániz, I.M.; Lizarbe-Sancha, S.; Arana, S.; Zhukova, V.; Mujika, M.; Zhukov, A. Glass-coated ferromagnetic microwire-induced magnetic hyperthermia for in vitro cancer cell treatment. *Mater. Sci. Eng. C* **2020**, *106*, 110261. [CrossRef]

20. Salaheldeen, M.; Garcia-Gomez, A.; Corte-León, P.; Gonzalez, A.; Ipatov, M.; Zhukova, V.; Gonzalez, J.M.; López Antón, R.; Zhukov, A. Manipulation of Magnetic and Structure Properties of Ni$_2$FeSi Glass-Coated Microwires by Annealing. *J. Alloys Compd.* **2023**, *942*, 169026. [CrossRef]

21. Salaheldeen, M.; Talaat, A.; Ipatov, M.; Zhukova, V.; Zhukov, A. Preparation and Magneto-Structural Investigation of Nanocrystalline CoMn-Based Heusler Alloy Glass-Coated Microwires. *Processes* **2022**, *10*, 2248. [CrossRef]

22. Salaheldeen, M.; Garcia-Gomez, A.; Corte-Leon, P.; Ipatov, M.; Zhukova, V.; Gonzalez, J.; Zhukov, A. Anomalous Magnetic Behavior in Half-Metallic Heusler Co$_2$FeSi Alloy Glass-Coated Microwires with High Curie Temperature. *J. Alloys Compd.* **2022**, *923*, 166379. [CrossRef]

23. Salaheldeen, M.; Ipatov, M.; Zhukova, V.; García-Gomez, A.; Gonzalez, J.; Zhukov, A. Preparation and magnetic properties of Co$_2$-based Heusler alloy glass-coated microwires with high Curie temperature. *AIP Adv.* **2023**, *13*, 025325. [CrossRef]

24. Salaheldeen, M.; Garcia, A.; Corte-Leon, P.; Ipatov, M.; Zhukova, V.; Zhukov, A. Unveiling the Effect of Annealing on Magnetic Properties of Nanocrystalline Half-Metallic Heusler Co$_2$FeSi Alloy Glass-Coated Microwires. *J. Mater. Res. Technol.* **2022**, *20*, 4161–4172. [CrossRef]

25. Salaheldeen, M.; Ipatov, M.; Corte-Leon, P.; Zhukova, V.; Zhukov, A. Effect of Annealing on the Magnetic Properties of Co$_2$MnSi-Based Heusler Alloy Glass-Coated Microwires. *Metals* **2023**, *13*, 412. [CrossRef]

26. Salaheldeen, M.; Wederni, A.; Ipatov, M.; Gonzalez, J.; Zhukova, V.; Zhukov, A. Elucidation of the Strong Effect of the Annealing and the Magnetic Field on the Magnetic Properties of Ni$_2$-Based Heusler Microwires. *Crystals* **2022**, *12*, 1755. [CrossRef]

27. Salaheldeen, M.; Garcia-Gomez, A.; Ipatov, M.; Corte-Leon, P.; Zhukova, V.; Blanco, J.M.; Zhukov, A. Fabrication and Magneto-Structural Properties of Co$_2$-Based Heusler Alloy Glass-Coated Microwires with High Curie Temperature. *Chemosensors* **2022**, *10*, 225. [CrossRef]

28. Ulitovsky, A.V.; Maianski, I.M.; Avramenco, A.I. Method of Continuous Casting of Glass Coated Microwire. USSR Patent 128427, 15 May 1960.

29. Salaheldeen, M.; Zhukova, V.; Wederni, A.; Ipatov, M.; Zhukov, A. Magnetic Properties of Co$_2$MnSi-based Heusler Alloy Glass-coated Microwires. *TechRxiv* **2023**. Preprint. [CrossRef]

30. Chiriac, H.; Lupu, N.; Stoian, G.; Ababei, G.; Corodeanu, S.; Óvári, T.A. Ultrathin Nanocrystalline Magnetic Wires. *Crystals* **2017**, *7*, 48. [CrossRef]

31. Salaheldeen, M.; Wederni, A.; Ipatov, M.; Zhukova, V.; Lopez Anton, R.; Zhukov, A. Enhancing the Squareness and Bi-phase Magnetic Switching of Co$_2$FeSi Microwires for Sensing Application. *Preprints.org* **2023**, 2023040071. [CrossRef]

32. Goto, T.; Nagano, M.; Wehara, N. Mechanical properties of amorphous Fe$_{80}$P$_{16}$C$_3$B$_1$ filament produced by glass-coated melt spinning. *Trans. JIM* **1977**, *18*, 759–764. [CrossRef]

33. Zhukova, V.; Cobeño, A.F.; Zhukov, A.; de Arellano Lopez, A.R.; López-Pombero, S.; Blanco, J.M.; Larin, V.; Gonzalez, J. Correlation between magnetic and mechanical properties of devitrified glass-coated Fe$_{71.8}$Cu$_1$Nb$_{3.1}$Si$_{15}$B$_{9.1}$ microwires. *J. Magn. Magn. Mater.* **2002**, *249*, 79–84. [CrossRef]

34. Talaat, A.; Alonso, J.; Zhukova, V.; Garaio, E.; García, J.A.; Srikanth, H.; Phan, M.H.; Zhukov, A. Ferromagnetic Glass-Coated Microwires with Good Heating Properties for Magnetic Hyperthermia. *Sci. Rep.* **2016**, *6*, 39300. [CrossRef]

35. Kozejova, D.; Fecova, L.; Klein, P.; Sabol, R.; Hudak, R.; Sulla, I.; Mudronova, D.; Galik, J.; Varga, R. Biomedical applications of glass-coated microwires. *J. Magn. Magn. Mater.* **2019**, *470*, 2–5. [CrossRef]

36. Wederni, A.; Ipatov, M.; Pineda, E.; Escoda, L.; González, J.-M.; Khitouni, M.; Suñol, J.-J. Martensitic Transformation, Thermal Analysis and Magnetocaloric Properties of Ni-Mn-Sn-Pd Alloys. *Processes* **2020**, *8*, 1582. [CrossRef]

37. Mitra, S.; Ahmad, A.; Chakrabarti, S.; Biswas, S.; Das, A.K. Investigation on Structural, Electronic and Magnetic Properties of Co$_2$FeGe Heusler Alloy: Experiment and Theory. *J. Magn. Magn. Mater.* **2022**, *552*, 169148. [CrossRef]

38. Óvári, T.-A.; Lupu, N.; Chiriac, H. Rapidly Solidified Magnetic Nanowires and Submicron Wires, Advanced Magnetic Materials. Malkinski, L., Ed.; InTech: London, UK, 2012; pp. 1–32, ISBN 978-953-51-0637-1.

39. Zhukova, V.; Blanco, J.M.; Ipatov, M.; Zhukov, A. Magnetoelastic contribution in domain wall dynamics of amorphous microwires. *Phys. B* **2012**, *407*, 1450–1454. [CrossRef]

40. Torcunov, A.V.; Baranov, S.A.; Larin, V.S. The internal stresses dependence of the magnetic properties of cast amorphous microwires covered with glass insulation. *J. Magn. Magn. Mater.* **1999**, *196–197*, 835–836. [CrossRef]

41. Besseghini, S.; Gambardella, A.; Chernenko, V.A.; Hagler, M.; Pohl, C.; Mullner, P.; Ohtsuka, M.; Doyle, S. Transformation behavior of Ni-Mn-Ga/Si(100) thin film composites with different film thicknesses. *Eur. Phys. J. Spec. Top.* **2008**, *158*, 179–185. [CrossRef]

42. Zhukov, A.; Ipatov, M.; del Val, J.J.; Zhukova, V.; Chernenko, V.A. Magnetic and structural properties of glass-coated Heusler-type microwires exhibiting martensitic transformation. *Sci. Rep.* **2018**, *8*, 621. [CrossRef] [PubMed]